Influence of particle zeta potential and experimental procedure on protein corona formation

and multicomponent aggregation

Aida López Ruiz¹, Mengyuan Xao², Asmitha Sathya³, Nicole Piccininni⁴, Guangliang Liu¹, Noshin

Siddiq⁵, Hao Chen², Kathleen McEnnis^{1*}

1. Department of Chemical and Materials Engineering, New Jersey Institute of Technology,

Newark, NJ, USA.

E-mail: mcennis@njit.edu

2. Department of Chemistry & Environmental Science, New Jersey Institute of Technology,

Newark, NJ, USA.

3. Department of Biomedical Engineering, Johns Hopkins University, Baltimore, MD, USA

4. Federated Department of Biological Sciences, New Jersey Institute of Technology, Newark, NJ,

USA.

5. Department of Chemical and Biomolecular Engineering, New York University, Brooklyn, NY,

USA.

Keywords: nanoparticle tracking analysis, protein corona, particle aggregation, polystyrene

nanoparticles

Abstract: Drug delivery systems have renewed attention in recent years to achieve targeted

delivery while decreasing toxic side effects. However, there are many factors that prevent optimal

administration of drug delivery particles. For instance, protein corona formation and aggregation

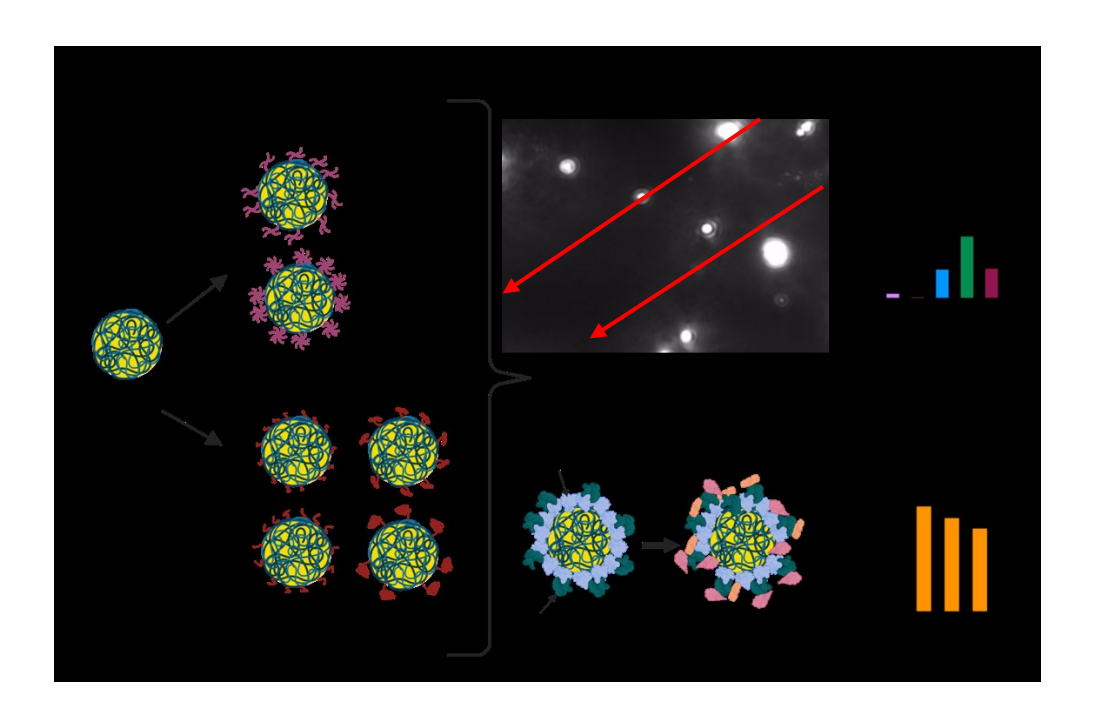
both decrease the circulation half-life of drug delivery particles, leading to sequestration to the

liver and spleen. Therefore, optimal surface modifications are needed to decrease protein corona

1

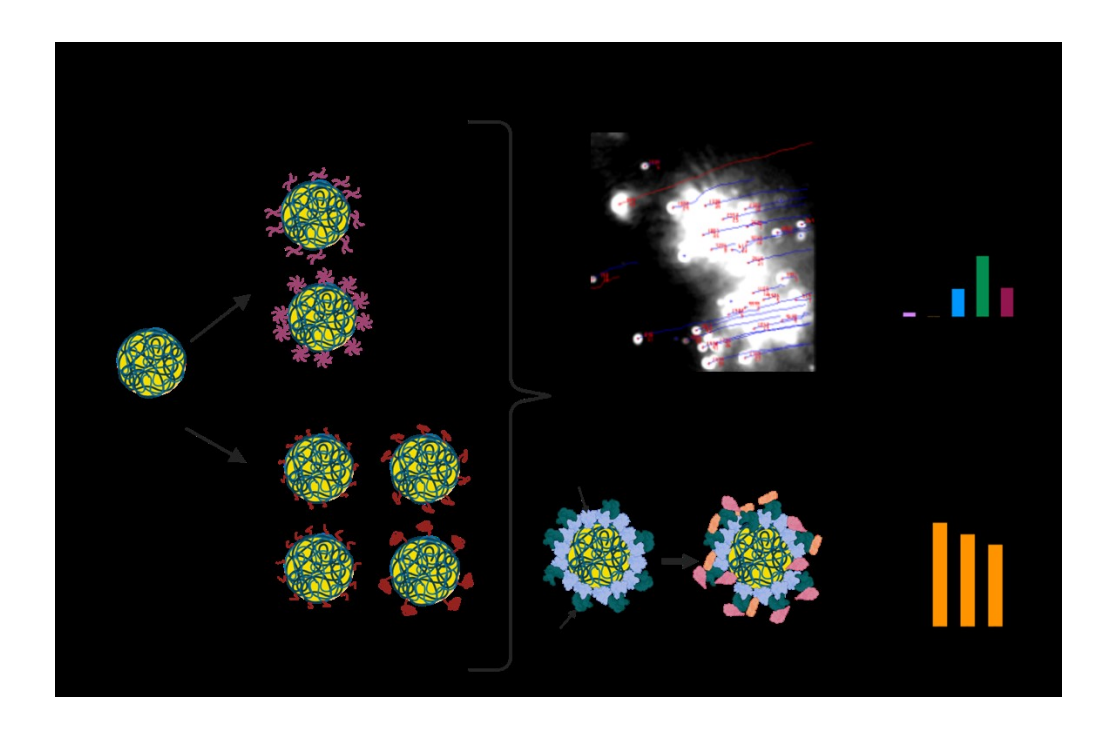
formation and avoid aggregation. In this work, polystyrene particles were modified with multiarm and linear polyethylene glycol (PEG) to determine their aggregation profiles and protein
corona formation. Multi-arm PEGs were found to aggregate more than linear PEGs, due to the
change in zeta potential from unreacted end groups, which may lead to shorter circulation halflives. Furthermore, the protein corona formation and composition were studied after different
washing procedures, highlighting the importance of studying protein corona formation with
undiluted blood plasma.

Graphical abstract with GIF:



Created with Biorender.

Graphical abstract with figure:



Created with Biorender.

Introduction

The use of nanoparticles for drug delivery is a growing field with potential to limit toxic side effects and decrease the amount of drug needed for treatment. Nanoparticle size is an important factor for a successful drug delivery system since varying size will vastly change the internalization of the particles by the cells. However, a major barrier that prevents the application of drug delivery systems in clinical trials is the protein corona formation on the nanoparticles. Nanoparticles that circulate in the bloodstream are rapidly recognized by proteins. Proteins attach to the surface forming a nanoparticle-protein complex (protein corona) that leads to phagocytic system recognition and removal from the bloodstream ¹. The protein corona is divided into two main components, the hard corona, and the soft corona ²⁻⁴. The hard corona is composed of proteins tightly bound to the surface of the particles while the soft corona is loosely bound to other proteins ⁵. The protein corona increases the particle size, decreasing internalization of the particles by the

cells. Moreover, when using targeting ligands on the surface of the particles, such as antibodies, the protein corona will produce a masking effect, preventing the ligands from finding the target cells ⁶. The presence of a protein corona can also cause nanoparticle aggregation, which reduces circulation time of the particles in the body ⁷.

The use of polymers on the surface of the particles to avoid the formation of a protein corona is therefore a common procedure. Polyethylene glycol (PEG) is frequently used on the surface since PEG can resist interactions with components from blood and stay inert 8. The hydrophilicity of PEG creates a hydrated layer surrounding the nanoparticle. This limits interactions between particles and blood components, preventing the protein corona formation ^{1,8}. Previous research has demonstrated that the use of PEG increases circulation time and reduces the accumulation in the liver compared with non-PEGylated particles ^{9,10}. There are several parameters of PEG that affect the dynamics of nanoparticles in blood. Molecular weight, surface density, and architecture have been found to be key parameters of PEG that need to be controlled to engineer a successful PEGylated drug delivery system 8,11,12. For instance, molecular weight will drastically change the protein adsorption on the surface. Previous studies have found that high molecular weight PEG leads to the aggregation of particles, while a molecular weight less than 2 kDaltons will have little effect on the circulation time ¹³. Many nanoparticles are surface modified with linear PEG; however, multi-arm star PEGs, generally with either 4, 6, or 8 arms, have been used for surface modifications to prevent protein adsorption and change diffusion behavior of nanoparticles compared to linear PEG ¹⁴⁻¹⁷. The use of multi-arm PEGs can lead to unreacted functional groups on the surface of the particles; therefore, zeta potential needs to be studied when modifying the surface with multi-arm PEGs. Hence, many considerations must be considered to achieve optimum circulation time and reduce aggregation behavior with blood components.

Protein corona characterization and aggregation behavior is usually performed by dynamic light scattering (DLS) ^{1,18-20}. However, DLS is a technique that requires a clear sample so light is scattered from the particles and no other components ²¹. Analyzing particle size in whole blood or undiluted plasma using DLS can only be accomplished for certain particles size ranges that do not overlap with the scattering from other components in the blood and requires complex curve fitting ^{18,22,23}. Moreover, the multicomponent aggregation behavior between particles and blood components cannot be studied with DLS. Hence, particles incubated in blood typically need to be washed to eliminate components that interfere with the scattering, resulting in the loss of proteins from the corona, effecting the measured protein corona size ²⁴. Consequently, other techniques such as nanoparticle tracking analysis (NTA), due to its unique visualization of the particle movement, can be used to characterize aggregation behavior and the size of the protein corona, without the need for washing or diluting the sample, resulting in a larger protein corona than reported for other methods ²⁴. Hence, experimental conditions have a large impact on characterization of the protein corona.

In this study, polystyrene (PS) nanoparticles surface modified with PEG of varying molecular weight, either linear or multi-armed with drastically different zeta-potentials (Figure 1A) were used to study protein corona and aggregation behavior with blood components. NTA was used to determine how these parameters on PS particles modified with PEG affect the formation of a protein corona and the aggregation behavior of the particles in blood plasma. Furthermore, the corona formation with undiluted plasma and different washing steps was analyzed to study the formation of soft vs hard corona.

Materials and methods

Materials

Bovine blood was purchased from Lampire Biological Laboratories (catalog# 7200806). FluoSpheres® carboxylate-modified polystyrene nanoparticles 200 nm in diameter labeled with a yellow-green dye (excitation 505 nm, emission 515 nm) were purchased from ThermoFisher (catalog# F8811). Amine terminated PEG of varying molecular weight and architecture, specifically 1k linear PEG (MW=1,000 g/mol, catalog# PG1-AM-1k), 5k linear PEG, (MW=5,000 g/mol, catalog# PG1-AM-5k), 10k linear PEG (MW=10,000 g/mol, catalog# PG1-AM-10k), 30k linear PEG (MW=30,000 g/mol, catalog# PG1-AM-30k), 4-arms 20k PEG (MW=20,000 g/mol, catalog# PG4A-AM-20k), and 8-arms 40k PEG (MW=40,000 g/mol, catalog# PG8A-AM-40k) were purchased from Nanocs. 1-Ethyl-3-(3-dimethylaminopropyl) carbodiimide-HCl (EDC) (catalog# 22981) and sulfo-N-hydroxysulfosuccinimide (NHS) (catalog# PI24510) were purchased from Thermo Scientific. Iodoacetamide (catalog# I1149) and urea (catalog# U6504) were purchased from Sigma Life Science. DL-Dithiothreitol (catalog# 43819), ammonium bicarbonate (catalog# 09830), and Amicon Ultra-0.5 centrifugal filter units with a 3kDa molecular weight cutoff (MWCO) (catalog# UFC5003) were purchased from Sigma-Aldrich. Proteomics grade trypsin (catalog# 3708969001) was purchased from Roche Diagnostics GmbH (Mannheim, Germany).

Blood Plasma Preparation

Whole bovine blood treated with the anticoagulant sodium citrate was centrifuged 3 times at 2000 RCF for 10 minutes to separate blood cells from the solution, obtaining blood plasma. Kinematic viscosity was measured using a glass capillary Ubbelholde viscometer (Fisher Scientific catalog# 13614F) in a water bath at 37°C.

PEGylation

A solution of 50 μL of polystyrene particles was resuspended in a solution of 1 mL of MES (2-(N-morpholino) ethanesulfonic acid) buffer solution and 0.4 mg EDC. The solution was vortexed and reacted at room temperature on a rotator for 10 minutes. After the particles reacted with EDC, 20 μL of a solution of 1.1 mg sulfo-NHS with 40 μL MES was added to the particle solution, vortexed, and reacted at room temperature on a rotator for 10-15 minutes. The particles were centrifuged at 22136 RCF for 1 hour at 4°C. Then, the supernatant was removed, and 1 mL of phosphate buffered saline (PBS) was added, and the sample was tip sonicated. 15 mg of PEG was added to the solution and reacted at room temperature on a rotator for 2 hours. PEG was added in excess to the dilute particle solutions to maximize the PEGylation reaction and, in the case of multi-armed PEG, to prevent crosslinking between particles. Finally, to remove the excess PEG, particles were washed three times by centrifuging at 22136 RCF for 1 hour, followed by replacing the supernatant with PBS. The molecular weights of the multi-arm PEGs were chosen such that an individual arm was of comparable molecular weight to the linear PEGs.

PEGylation of the particles was studied by measuring z-potential. For this process, 1 mL of each of the particle samples, with a minimum concentration of particles of 10⁹ particles/mL, was used for z-potential measurements using a Zetasizer nano ZS, Malvern Instrument to compare the z-potential of unmodified particles to PEGylated particles. Successful PEGylation was also confirmed by ¹H nuclear magnetic resonance spectroscopy (NMR, Bruker AVIII-500). For NMR measurements, PEGylated particles were freeze dried and ~ 1 mg of dried particles was dissolved in deuterated chloroform (0.6 ml).

Multicomponent Aggregation Experiment

Particles were incubated with undiluted plasma at 37°C rotating at 25 RPMs. After 10 minutes of incubation, the first measurement was conducted. A 10 minute incubation period was selected to

allow formation of the initial protein corona on all the particles, while still performing the size measurement before significant protein exchanges in the protein corona occur, which begin after several hours of incubation ². 1mL of sample was retrieved from the incubation tube for NTA analysis, conducted using a NanoSight NS300. The particles were incubated in the blood plasma continuously for 24 hours rotating inside of the incubator, and a 1 mL sample was taken at different time points throughout 24 hours. To investigate the aggregation of the different samples, the videos were analyzed to count the total number of particles in aggregates. Results were then normalized by the total number of particles in order to account for varying concentrations in each sample. The same blood sample was used for all the NTA experiments to be able to make comparisons across groups by minimizing patient to patient variability. Every time point included seven one-minute videos, to account for differences between runs.

Washing Experiments

Particles were incubated with undiluted plasma for 10 minutes at 37°C. The first measurement was conducted after the 10-minute incubation period using NTA (NanoSight NS300) to be consistent with the multicomponent aggregation experiments. After the first measurement, the particles were centrifuged at 22136 RCF for 30 min and the supernatant was replaced with normal saline (0.9% saline). After completing this washing step three times, the particle diameter was analyzed using NTA. Finally, two more washing steps were performed by centrifuging the particles at 22136 RCF for 30 min and replacing the supernatant with saline. The final measurement after five washing steps was done with NTA. The same blood sample was used for all the NTA experiments to minimize patient to patient variability that may occur. Every experiment was repeated three times, recording seven one-minute videos for each measurement.

Liquid chromatography/mass spectrometry (LC/MS) analysis

Nanoparticles were incubated in undiluted plasma for 10 minutes, followed by 5 washing steps. The remaining nanoparticle sample was vacuum dried to remove water. To denature the proteins in the particle sample, 200 µL of 8 M urea solution was added to each sample and agitated for 30 min to redissolve the protein. Then the proteins in the sample solution were reduced with 8.6 µL of 500 mM dithiothreitol (DTT) and alkylated by 17.1 µL of 500 mM iodoacetamide (IAA) for 30 min at room temperature in the dark. Then 8.6 µL of 500 mM DTT was added again to quench the excess IAA. The resulting solution was then centrifuged at 4000 RCF for 4 min (room temperature) to separate nanoparticles from the protein solution. After centrifuging, 150 μL of the supernatant from the top of the tube containing protein solution, was taken for subsequent processing. The solution was placed in a 3kDa MWCO centrifugal filter (Amicon Ultra – 0.5 mL, Merck Millipore Ltd. Tullagreen, Carrigtwohill, Co Cork) and centrifuged at 14000 RCF for 30 min at room temperature. The sample was subsequently washed three times with 400 µL of 50 mM ammonium bicarbonate (ABC) buffer to remove the urea and excess DTT. After washing, the filter was placed upside-down in centrifuge tubes and centrifuged at 4000 RCF for 3 min (room temperature) to transfer and collect all the protein sample in the filter. The resulting protein sample was reconstituted in 200 μL of 50 mM ABC buffer. For protein digestion, 10 μL of trypsin (0.5 μg/μL Roche) was added and incubated with the sample at 37 °C overnight (15h to 17h). The digestion reaction was quenched with 1 μL of formic acid, and 10 μL of the resulting peptide solution was taken and diluted with 40 µL of acetonitrile/water/formic acid (ACN/H₂O/FA, 50/50/0.1, v/v/v) for LC/MS analysis ²⁵.

All LC/MS experiments were performed using ultraperformance liquid chromatography (UPLC, Waters, Milford, MA) coupled with a high-resolution Orbitrap Q Exactive mass spectrometer (Thermo Scientific, San Jose, CA). A reversed phase column (BEH C18, 2.1 mm ×

50 mm, $1.7 \text{ }\mu\text{m}$) was used for peptide separation of the protein digest mixture with a mobile phase flow rate of $200 \text{ }\mu\text{L/min}$. Mobile phase A (water with 0.1% formic acid) and mobile phase B (acetonitrile with 0.1% formic acid) were used for LC separation. In the elution gradient, mobile phase B was initially set to 5% of the total mobile phase from 0-3 min and increased to 35% from 3 min to 40 min. Then mobile phase B climbed to 95% in 5 min and was held at 95% for 5 min, before being reduced to 5% at 55 min. To reach equilibrium in the column between runs, the mobile phase was then held at 95% mobile phase A and 5% mobile phase B for 3 minutes at the end of each measurement.

After peptide separation, a heated electrospray ionization (HESI) source was used to ionize the eluted peptides with a sheath of nitrogen (30 L/h). The source temperature and ionization voltage were 300°C and +4 kV, respectively. Data-dependent acquisition (DDA) MS/MS was performed where the first event was the survey positive mass scan (m/z range of 250–1800), followed by 20 higher-energy C-trap dissociation (HCD) events (30% normalized collision energy, NCE) on the 20 most abundant ions detected from the first event. Resolution for MS/MS analysis was set to 70,000 (AGC target of 3E6) and 17,500 (AGC target of 5E4) for survey scans and (HCD) scans ²⁶. Mass spectra was recorded using Thermo Xcalibur, and raw data was analyzed using Thermo Proteome Discoverer (PD) 2.4. A database FASTA file was generated from Uniport under a search of bovine plasma (33000+ entries).

Statistical Methods

Statistical analysis was performed by one-way ANOVA, complimented with Tukey's post-test. The data was considered statistically significant when p-values were <0.05; (*p <0.05, **p <0.01, ***p <0.001; ****p <0.0001), and p-values of >0.05 were considered not significant (ns).

Results and discussion

Characterization

The use of fluorescent particles facilitates the study of the interaction between blood components and the particles using NTA. For these studies, six different surface modifications with PEG were performed on the surface of fluorescent PS particles. The surface modifications were classified based on the architecture of the PEG used and the molecular weight. Therefore, the particles were classified as: 1K (1000 g/mol), 5K (5000 g/mol), 10K (10,000 g/mol), 30K (30,000 g/mol), 4-arm (20,000 g/mol) and 8-arm (40,000 g/mol) (Figure 1A). The size in saline of all the particles was studied using NTA (Figure 1 B and C, Figure S1). The size of the PS particles significantly increased for all the different PEG conformations except for 1K. To further characterize the presence of PEG on the surface, z-potential was used, where a statistically significant increase in z-potential was observed for PEGylated particles (Figure 1D). Specifically, for 4-arms and 8-arms, due to the abundance of unreacted amine groups, a drastic increase in z-potential was observed compared to unmodified PS. Characterization by NMR was also performed where the peak at 3.6 ppm, corresponding to the methylene protons of the PEG backbone, confirmed the presence of PEG (Figure 1E, Figure S2). By comparing the integration of the PEG methylene proton peak to the peak for PS's aromatic protons, the weight percentage of PEG on each particle was characterized (Table S1).

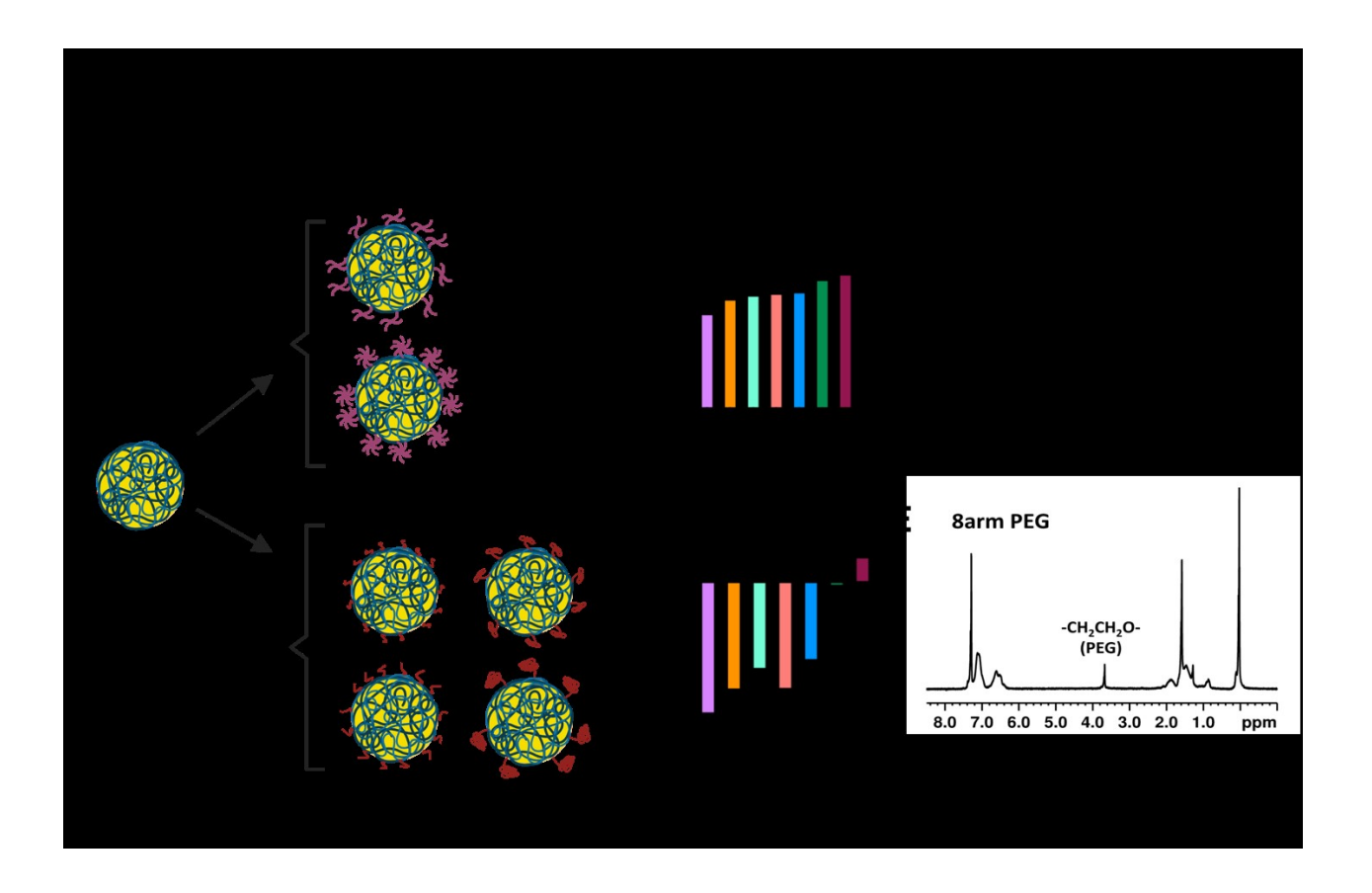


Figure 1. A) Schematic representation of different surface modifications with PEGs on the surface of PS particles. B) Size analysis of PS particles in saline with different surface modifications. C) Size representation using NTA of 5K particles in saline. D) Z-potential of the different particles studied after performing surface modifications. E) NMR spectra showing PEG on the surface of the particles. Created with Biorender.

Multicomponent aggregation

Particle aggregation is a frequent issue with many nanoparticles. However, nanoparticles are often only analyzed for their aggregation with each other, i.e. particle-particle aggregation. It is well known that salt content can trigger aggregation of particles, so size measurements of particles in saline are often done to confirm the particles do not aggregate with each other. However, multicomponent aggregation of particles is rarely investigated. Multicomponent aggregation is

when more than one particle aggregates with components of the surrounding solution (in this case the blood plasma), rather than aggregating with other particles (Figure 2) ²⁴. Drug delivery vehicles will encounter many different proteins when used for clinical applications, so it is important to determine the multicomponent aggregation of drug delivery particles with the components of blood as aggregation with these components could dramatically decrease the circulation half-life of the particles in the body.

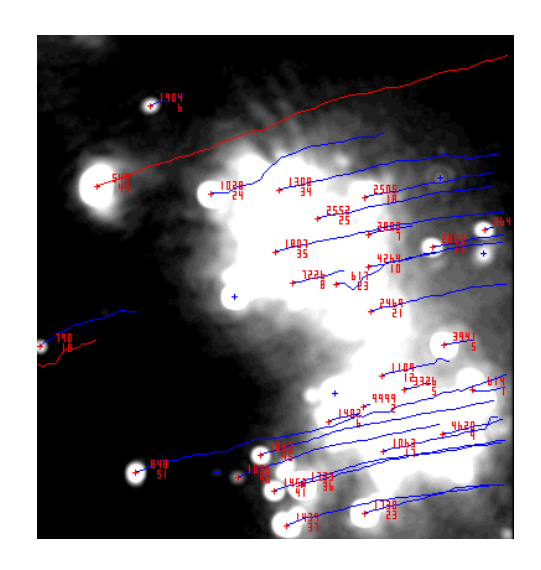


Figure 2. Screenshot of an aggregate of particles with blood components creating a multicomponent aggregate analyzed with NTA after 24h incubation of PS particles with blood plasma. Particle tracks are indicted by the red and blue lines, with particles in the multicomponent aggregate moving together without the Brownian motion seen in individual particles.

In this study, therefore, the multicomponent aggregation of the particles was studied over a 24-h period for unmodified PS, and PS particles modified with linear 1K, linear 30K, 4-arm star, and 8-arm star PEG in undiluted plasma. For this experiment, linear 5K and 10K PEG were not included as they were analyzed in a previous study ²⁴. Figure 3 presents the observed multicomponent aggregation behavior of particles with blood components at different time points for each surface modification tested. The number of particles in aggregates is defined as the

number of particles centers found to be moving together without Brownian motion, indicating that the particles are in a multicomponent aggregate with blood components ²⁴. The number of particles in aggregates is normalized to account for the total number of particles counted in that measurement. In this work multicomponent aggregation behavior is presented for each time point to highlight the variation between times as well as the overall multicomponent aggregation to compare to previous studies. Multicomponent aggregation begins to peak in most samples after 4 or 8 hours in blood plasma, with several samples showing additional peaks in multicomponent aggregation again around 24 hours. The change in multicomponent aggregation behavior at different time points may be explained by changes in the protein corona over time. Initially the protein will be mostly made of proteins with the greatest abundance in the blood plasma (albumin), however, over time, typically on the order of several hours, the proteins in the protein corona will be replaced by proteins with a higher affinity for the particle surface ². The proteins in the protein corona, specifically fibrinogen, are likely triggering the observed multicomponent aggregation, so changes in the protein corona will change the aggregation behavior. Protein affinity for the particles will be strongly influenced by the particle's z-potential, therefore differences in zpotential will affect which proteins are in the protein corona and their affinity with other proteins. The variation in multicomponent aggregation over time is likely linked to protein corona changes, since the affinity between proteins may lead to a higher number of particles in multicomponent aggregates at different time points.

A drastic change in the scale of the number of particles in multicomponent aggregates can be observed when linear 1K PEG particles are compared to the multi-arm PEGs used, 4-arm and 8-arm. The maximum number of particles in aggregates for 1K PEG particles was 210 particles per 1x10⁵ particles, while for 4-arm PEG particles, the maximum was 4894 particles in aggregates

per 1x10⁵ particles, an increase of more than 20 times. Furthermore, for 8-arm PEG particles, the maximum number of particles in aggregates per 1x10⁵ particles was 1869, around 10 times more aggregation than for 1K PEG. This aggregation behavior for multi-arm PEG can be explained by the presence of the unreacted amine end groups on the PEG arms that change the charge on the surface of the particles into a more neutral charge (Figure 1D). As particles become more neutral, there is a decrease in the electrostatic repulsive forces keeping the particles dispersed, and particleparticle aggregation is more likely ²⁷. For linear PEG there is only one amine group on the end of the chain that is reacted via EDC-NHS chemistry to attach the PEG chain to the surface carboxylic groups on the PS particles. However, for multi-arm PEG's each of the arms have an amine end group. The PEG is present in excess during PEGylation reactions to ensure there is no crosslinking between particles, meaning that each multi-arm PEG is likely connected to the PS particle by only one arm, leaving the remaining arms with unreacted amine groups, conferring an almost neutral or slightly positive charge that triggers excessive aggregation. The use of multi-arm star PEG on the surface of drug delivery particles must be done with consideration for the type of end-group and the extent of any subsequent reactions, because of its effects on the surface charge and resulting multicomponent aggregation behavior of the particles.

To further compare the multicomponent aggregation behavior of the particles to previous studies, the average number of particles in aggregates over the 24-hour time period was compared for each surface modification (Figure 3 F). It can be observed that 1K PEG had on average less multicomponent aggregation than unmodified particles. Additionally, both multi-arm PEGs and 30K PEG showed more multicomponent aggregation compared to 1K PEG. The behavior of both sets of multi-arm PEG can be explained by the higher z-potential as previously mentioned. However, the behavior of 30K PEG was not expected as in previous aggregation studies with goat

blood plasma the 30K PEG modified particles were found to be statistically similar to other linear PEGs ²⁴. In this previous study, however, not only was the species of blood plasma different (goat versus bovine in this study), but the anticoagulant used was also different (Alsever's solution versus sodium citrate in this study). These differences may account for the discrepancies and indicate the importance of the experimental study details when analyzing the multicomponent aggregation behavior and protein corona. The change in the aggregation behavior could also be attributed to a different patient sample. Protein concentrations can vary patient to patient, and these variations may result in large discrepancies in the aggregation behavior; therefore, the protein composition of the corona needs to be examined to account for patient to patient variation. Furthermore, these results indicate that aggregation behavior in nanomedicine may be patient specific and require a personalized medicine approach.

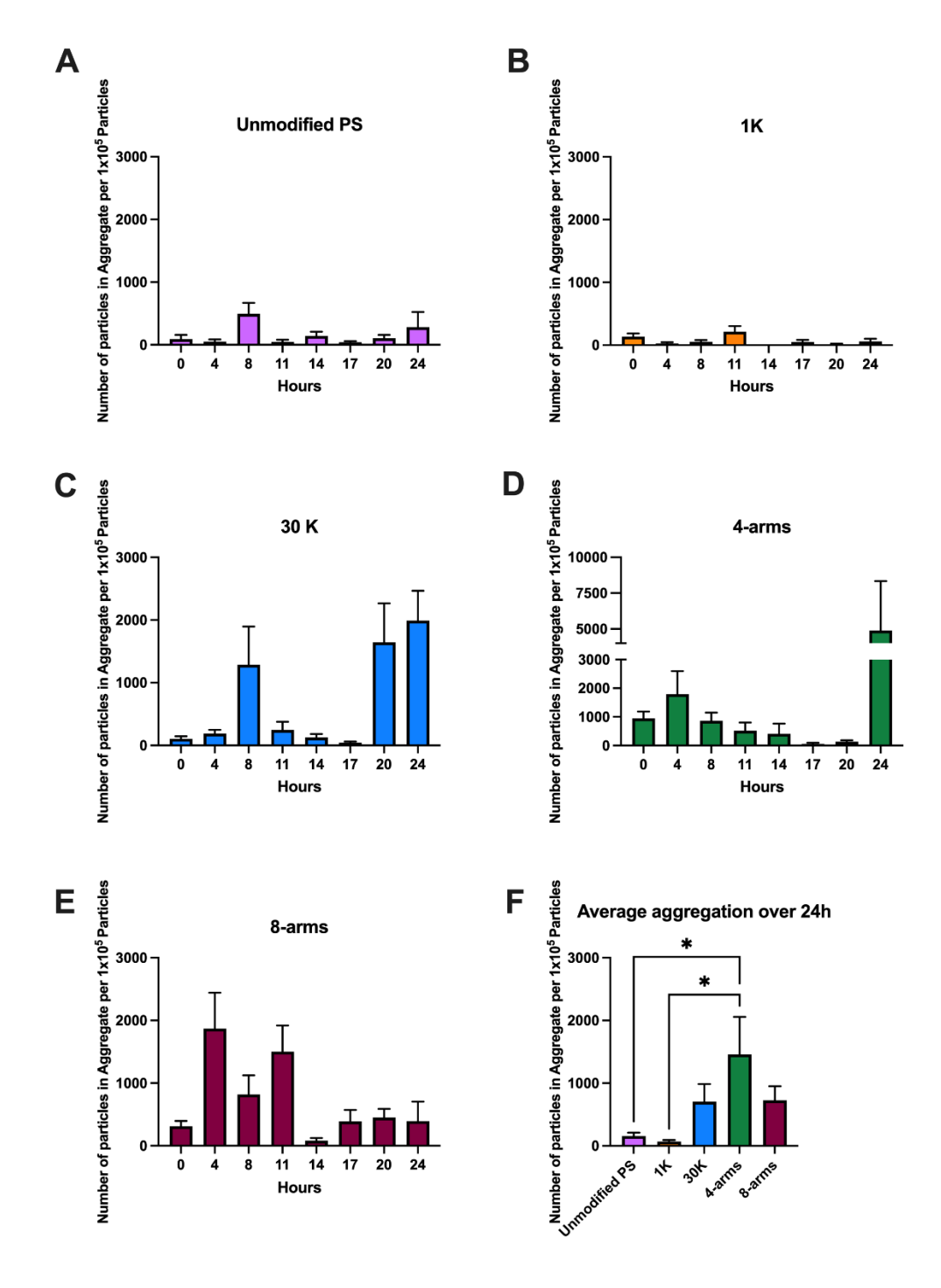


Figure 3. Quantification of number of particles in multicomponent aggregates (particles aggregated with blood components) per 1 x 10⁵ particles per time point. A) Unmodified PS particles, B) 1K PEG, C) 30K PEG, D) 4-arm PEG, E) 8-arm PEG and F) Quantification of number of particles in multicomponent aggregates per 1 x 10⁵ particles averaged for all the time points.

Displayed error bars represent standard error for each time point. * Is a significance level of 95% with p-value< 0.05.

Protein corona formation

The protein corona has been hypothesized to follow a hard/soft corona model, where the proteins in the soft corona are loosely bound and more readily desorbed and adsorbed from the particle surface ^{2,3,6}. Hence, the use of washing steps or the dilution of the plasma solution can cause the loss of the soft corona components, resulting in a smaller thickness of the protein corona. Therefore, in this study the protein corona thickness in undiluted plasma and after washing steps was measured. NTA measurements were performed with all the sets of particles after different washing steps, however, due to the extensive particle-particle aggregation behavior of 4-arm and 8-arm PEG particles (Figure S3) the thickness of the protein corona was not possible to study as a peak corresponding to individual particles could not be discerned in the size distribution.

After 10 minutes of incubation of the particles in undiluted bovine plasma, an initial size analysis was performed in the undiluted blood plasma to characterize the full protein corona. Afterwards, the particles were subjected to several washing steps by centrifuging, removing the supernatant, and adding normal saline solution. After 3 and 5 washing steps, the size was analyzed again and a decrease in size was observed (Figure 4). Interestingly, a clear difference between soft and hard corona was not perceived, and a gradual decrease was observed instead. Particles with 1K PEG displayed statistically significant differences in size for each of the washing steps, decreasing in size after each wash, suggesting a gradient of proteins bound to the surface as opposed to a two-layer formation (Figure 4 A). On the other hand, 5K, 10K and 30K PEG particles displayed the same trend as 1K but with significant differences between the unwashed particles and after different washing steps (Figure 4 C, D), with the exception of 5K PEG which did not

show any significant differences in size. The trend observed in all sets of particles suggests a gradient of proteins bound on the surface of the particles with different affinities depending on the molecular weight of PEG. Furthermore, it has been demonstrated that the proteins on the surface of the particles each have their own adsorption and desorption rates ^{4,28}, therefore, it is possible that there is no clear hard and soft corona structure and different PEG modifications will bind different types of proteins with varying affinities and desorption rates, creating a gradient protein corona rather than a distinct layered protein corona.

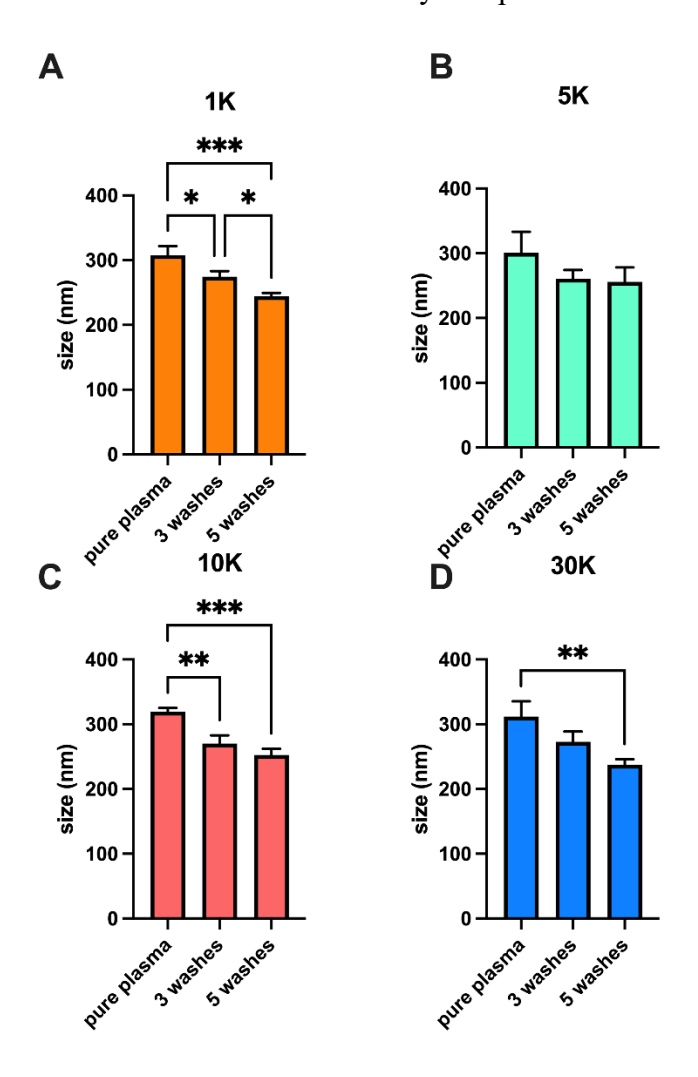


Figure 4. Particle size of PS PEGylated particles with A) 1K, B) 5K, C) 10K and D) 30K linear PEG. Pure plasma: size in undiluted plasma without washing, 3 washes: particle size after 3

washes, and 5 washes: particle size after 5 washes. * Is a significance level of 95% with p-value< 0.05, ** is a significance with p-value< 0.01, and *** is a significance with p-value< 0.001.

After particle size analysis, protein corona thickness was calculated by comparing the initial size of the particles in saline to the size of the particles incubated in undiluted plasma and the particle size after subsequent washing steps. In Table 1 the protein corona thickness is described for all the surface modifications and the different washing steps. Corona thickness after 5 washes was not calculated for unmodified PS particles, due to loss of particles after the washing steps, likely due to the difficulty resuspending PS particles without surface modifications (Table S2). When comparing protein corona thickness between the different groups, no statistically significant differences were found, however, a decrease in protein corona thickness after three washes was observed, indicating the removal of loosely bound proteins. To further understand the differences of the protein corona on various PEG modified particles, the protein corona composition was analyzed using mas-spectroscopy.

Table 1. Protein Corona Thickness (nm) after Different Washing Steps

	pure plasma	3 washes	5 washes		
Unmodified PS	56.9 ± 9	42.3 ± 3.2			
1K	58.7 ± 7	42 ± 4.3	27.1 ± 2.4		
5K	51 ± 16.1	31.1 ± 6.5	28.6 ± 11.1		
10K	61.8 ± 2.8	37.1 ± 6.3	28.3 ± 4.8		
30K	53.2 ± 11.7	33.6 ± 7.97	16 ± 4.2		

Protein corona composition

Protein corona composition was studied by using high resolution mass spectrometry (MS). This technique has previously been used to study the makeup of the protein corona ²⁹⁻³¹. From the list of proteins identified, 4 were found to have a major presence on the surface of the particles, as shown by the protein sequence coverage (%) in Table 2. All identified proteins can be found in Tables S3-S9. Protein sequence coverage (%) was calculated by dividing the length of identified peptide with total length of master protein. A higher coverage does not imply a higher concentration of protein, but rather how much of the protein sequence was found and identified in the sample.

Table 2. Four major proteins identified by Proteome Discoverer (PD): albumin, immunoglobin heavy constant mu (IGHM), β -2-glycoprotein 1, fibrinogen gamma-B chain (fibrinogen). Protein coverage was compared for each sample and represents percentage of the total protein sequence that was identified in each sample. ND=not detected.

		Coverage [%]						
Protein	Function	Unmodified PS	1K	5K	10K	30K	4-arms	8- arms
Albumin	Regulates osmotic pressure and binds to/transports many important small molecules through the blood	23	32	28	20	40	14	38
IGHM	Critical for immune response	10	17	17	10	45	9	15

ß-2-glycoprotein 1	Involved in blood clotting and lipid metabolism. Potentially plays a role in immune response.	3	10	10	3	8	3	3
Fibrinogen	Necessary for blood clotting and implicated in other processes like inflammation, wound healing, and angiogenesis	11	8	5	ND	3	ND	6

Albumin, which makes up more than 50% of plasma proteins, was present in the protein coronas of the nanoparticles for all sample groups. Albumin is essential in regulating cell osmotic pressure and binding salts, acids, water, vitamins, and hormones and carrying them between cells and tissues ³². As it is the most abundant protein in blood, it is typically detected in protein coronas ³³. Immunoglobulin heavy constant mu was also found in the protein coronas from all particle samples and is critical for immune response ³⁴. β-2-glycoprotein 1, which was present in the protein coronas of all the particles, is involved in the regulation of blood clotting and lipid metabolism ³⁵. It is also believed to be involved in immune response, but its role in the immune system is not yet fully understood. Lastly, fibrinogen gamma-B chain was detected in the protein coronas of all particles except for particles modified with 10k linear PEG and 4-arm star PEG. This protein is a component of the fibrinogen molecule, which is integral in blood coagulation ³⁶. It is involved in

clot formation and it has been implicated in other processes, like inflammation, wound healing, and angiogenesis.

High resolution LC/MS analysis was also performed for relative quantification of these four unique proteins across the different particle groups. This powerful technique provides high sensitivity and accuracy in peptide quantification. Peptides with the highest MS signal response were chosen for quantification. Results are displayed in Figure 5 and listed in Tables S2-S8. By analyzing with Thermo Xcalibur, an extracted ion chromatogram (EIC) for each peptide was generated as well as the peak area corresponding to each peptide. A higher EIC area corresponds to a higher concentration of that protein. Based on the LC/MS/MS results for all four proteins analyzed, a higher concentration of protein was found on particles modified with 30K linear PEG compared to particles modified with 1K linear PEG. Concentrations of protein for particles modified with 5K and 10K linear PEG are similar. Overall, 30K linear PEG modified particles had the highest protein concentration compared to the other surface modifications. Three out of the four analyzed proteins have a higher peptide concentration for 8-arm star PEG modified particles than 4-arm star PEG. Therefore, it may be concluded that the 30K linear PEG resulted in more adsorbed protein than 1K linear PEG, and that 8-arm star PEG had more adsorbed proteins than 4arm star PEG. Interestingly, the unmodified PS particles generally had less of the analyzed proteins than the particles with PEG modified surfaces. This may be due to the presence of surfactant on the surface of the as-received PS nanoparticles from the manufacturing process that may be limiting the adherence of proteins more effectively than PEG. Notably, the unmodified PS particles still contained fibringen in their protein corona, so would likely still trigger the clotting cascade despite the overall lack of proteins, thus emphasizing the importance of analyzing the protein corona in blood plasma rather than serum to understand the role of fibringen ³⁷.

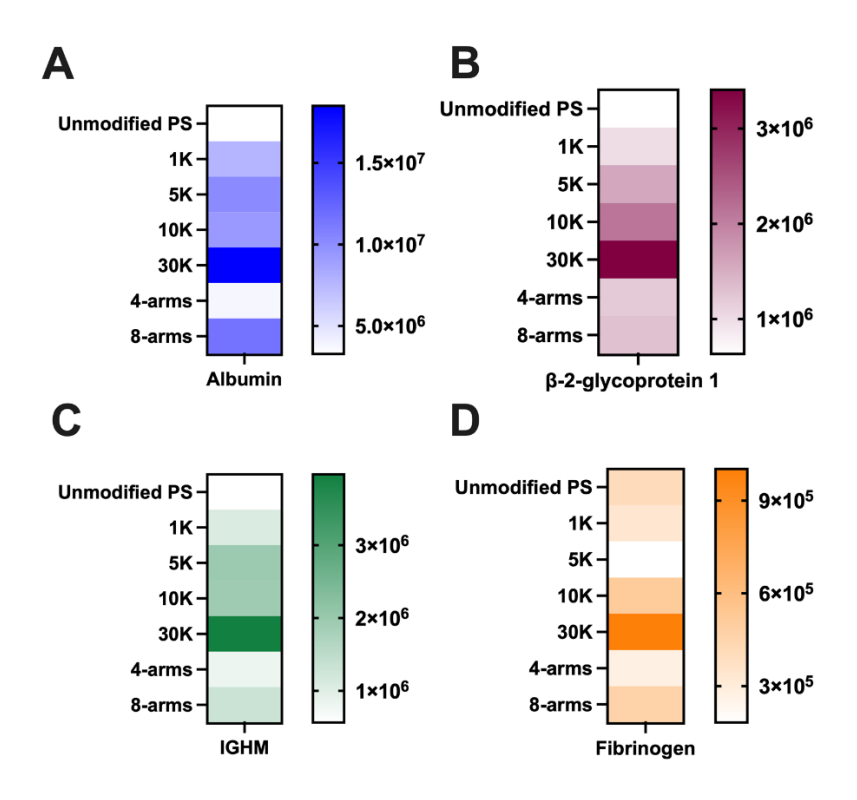


Figure 5. EIC peptide peak area comparison across particle groups: A) albumin, B) immunoglobulin heavy constant mu (IGHM), C) β-2-glycoprotein 1 and D) fibrinogen gamma-B chain.

Conclusions

The use of drug delivery systems, and specifically the use of polymeric drug delivery particles, to deliver therapeutic agents is a growing field. However, there are many barriers that prevent the particles from reaching the target cells, limiting the number of drug delivery systems that reach clinical trials. A major barrier for drug delivery vehicles is the formation of a protein corona. Since the apparent properties of the protein corona can vary depending on the conditions tested in, the protein corona formation needs to be characterized in physiological conditions. In this study we have demonstrated the importance of understanding multicomponent aggregation between particles and blood components, and the variations between types of PEGs on the surface. A larger

protein corona on the surface of particles may induce more multicomponent aggregation since affinities between proteins on the surface of the particles could trigger this multicomponent aggregation between particles and blood components ²⁴. Furthermore, it is important to characterize not just the particle size in blood but also the aggregation behavior with proteins since these large multicomponent aggregates could also trigger the immune system to remove these delivery particles from circulation. Multi-arm PEGs have previously been found to minimize protein interaction^{14,17}; however, it was found in this study that while there are not as many proteins on the surface, their aggregation behavior makes them underperform when tested in blood plasma. Furthermore, the protein corona thickness was not evaluated for 4-arm and 8-arm star PEG due to their excessive aggregation in blood plasma caused by their raised z-potential from the unreacted amine groups. In some instances, star-PEG is used without further modifications to the PEG arms¹⁵, however, even with further modifications, it is difficult to completely react all amine groups due to the steric hinderance in the dense PEG layer. Hence, the number and type of unreacted end groups need to be considered when designing surface modifications, since particles with a positive or neutral charge will aggregate more than negatively charged particles, such as particles modified with 1K linear PEG. With regards to the protein corona thickness and composition, by studying the particle size at different washing steps it was observed that the protein corona is a continuum layer as opposed to the commonly describe two layer 'soft' and 'hard' corona. Therefore, by washing the particles to study their protein corona there is a loss of proteins, and the degree of protein loss varies depending on the number of washing steps. Analysis of a reduced protein corona may lead to incorrect conclusions when comparing to the in vivo behavior of the particles. Furthermore, by analyzing the protein composition on the surface of the different particles studied, it could be observed that particles modified 30K linear PEG were found to have

a larger number of total proteins on the surface, in agreement with the multicomponent aggregation studies. However, this behavior may be patient specific or vary between species type or anticoagulant type. Hence, molecular weight and number of unreacted functional groups of PEG is important when designing drug delivery systems. This work provides insight into the variations between PEG modifications when studying their behavior in blood and highlights the importance of experimental design to obtain better drug delivery systems that can be used in clinical trials.

AUTHOR CONTRIBUTIONS

Aida López Ruiz: Conceptualization (lead); writing-original draft (lead), investigation (lead), formal analysis (lead). Mengyuan Xao: investigation (lead), writing-original draft (equal). Asmitha Sathya: investigation (lead), writing-original draft (equal). Nicole Piccininni: investigation (lead), writing-original draft (equal). Guangliang Liu: investigation (supporting), writing-original draft (equal). Noshin Sidiqq: investigation (supporting). Hao Chen: writing-review and editing (supporting); project administration (lead); resources (lead); supervision (lead). Kathleen McEnnis: Conceptualization (equal); project administration (lead); resources (lead); supervision (lead); writing-review and editing (lead).

ACKNOWLEDGEMENTS

The authors would like to thank the support of the NSF REU programs for support of AS (EEC-1560131) and for support of NS (EEC-2150369). MX and HC are thankful to the support of NSF (CHE-2203284)

CONFLICT OF INTEREST STATEMENT

The authors declare no conflicts of interest.

DATA AVAILABILITY STATEMENT

Data available in article supplementary material.

ORCID

Aida López Ruiz: https://orcid.org/0000-0003-1936-611X

Hao Chen: https://orcid.org/0000-0001-8090-8593

Kathleen McEnnis: https://orcid.org/0000-0001-7894-8641

REFERENCES:

1. Tenzer S, Docter D, Kuharev J, et al. Rapid formation of plasma protein corona critically

Nanotechnology. nanoparticle pathophysiology. 2013;8(10):772-781. affects Nature

doi:10.1038/nnano.2013.181

2. Rahman M, Laurent S, Tawil N, Yahia LH, Mahmoudi M. Nanoparticle and Protein

Corona. Springer Berlin Heidelberg; 2013:21-44.

3. Weiss ACG, Kempe K, Förster S, Caruso F. Microfluidic Examination of the "Hard"

Biomolecular Corona Formed on Engineered Particles in Different Biological Milieu.

Biomacromolecules. 2018;19(7):2580-2594. doi:10.1021/acs.biomac.8b00196

4. Mahmoudi M, Landry MP, Moore A, Coreas R. The protein corona from nanomedicine to

environmental science. Nature Reviews Materials. 2023;doi:10.1038/s41578-023-00552-2

5. Schäffler M, Semmler-Behnke M, Sarioglu H, et al. Serum protein identification and

quantification of the corona of 5, 15 and 80 nm gold nanoparticles. Nanotechnology. 2013/06/04

2013;24(26):265103. doi:10.1088/0957-4484/24/26/265103

Nguyen VH, Lee B-J. Protein corona: a new approach for nanomedicine design. 6.

International Journal of Nanomedicine. 2017; Volume 12:3137-3151. doi:10.2147/ijn.s129300

27

- 7. Pearson RM, Juettner VV, Hong S. Biomolecular corona on nanoparticles: a survey of recent literature and its implications in targeted drug delivery. Mini Review. Frontiers in Chemistry. 2014-November-27 2014;2doi:10.3389/fchem.2014.00108
- 8. Suk JS, Xu Q, Kim N, Hanes J, Ensign LM. PEGylation as a strategy for improving nanoparticle-based drug and gene delivery. Advanced Drug Delivery Reviews. 2016;99:28-51. doi:10.1016/j.addr.2015.09.012
- 9. Gref R, Minamitake Y, Peracchia MT, Trubetskoy V, Torchilin V, Langer R. Biodegradable long-circulating polymeric nanospheres. Science. Mar 18 1994;263(5153):1600-3. doi:10.1126/science.8128245
- 10. Klibanov AL, Maruyama K, Torchilin VP, Huang L. Amphipathic polyethyleneglycols effectively prolong the circulation time of liposomes. FEBS Lett. Jul 30 1990;268(1):235-7. doi:10.1016/0014-5793(90)81016-h
- 11. Bertrand N, Grenier P, Mahmoudi M, et al. Mechanistic understanding of in vivo protein corona formation on polymeric nanoparticles and impact on pharmacokinetics. Nature Communications. 2017;8(1)doi:10.1038/s41467-017-00600-w
- 12. Verhoef JJF, Anchordoquy TJ. Questioning the use of PEGylation for drug delivery. Drug Delivery and Translational Research. 2013;3(6):499-503. doi:10.1007/s13346-013-0176-5
- 13. Owens DE, Peppas NA. Opsonization, biodistribution, and pharmacokinetics of polymeric nanoparticles. International Journal of Pharmaceutics. 2006/01/03/ 2006;307(1):93-102. doi:https://doi.org/10.1016/j.ijpharm.2005.10.010
- 14. Cahn D, Duncan GA. High-Density Branched PEGylation for Nanoparticle Drug Delivery. Cellular and Molecular Bioengineering. 2022;15(5):355-366. doi:10.1007/s12195-022-00727-x

- 15. Rahmani S, Villa CH, Dishman AF, et al. Long-circulating Janus nanoparticles made by electrohydrodynamic co-jetting for systemic drug delivery applications. Journal of Drug Targeting. 2015;23(7-8):750-758. doi:10.3109/1061186x.2015.1076428
- 16. Amirgoulova EV, Groll J, Heyes CD, et al. Biofunctionalized Polymer Surfaces Exhibiting Minimal Interaction towards Immobilized Proteins. ChemPhysChem. 2004;5(4):552-555. doi:https://doi.org/10.1002/cphc.200400024
- 17. Song J, Ju Y, Amarasena TH, et al. Influence of Poly(ethylene glycol) Molecular Architecture on Particle Assembly and *Ex Vivo* Particle–Immune Cell Interactions in Human Blood. ACS Nano. 2021;15(6):10025-10038. doi:10.1021/acsnano.1c01642
- 18. Rausch K, Reuter A, Fischer K, Schmidt M. Evaluation of Nanoparticle Aggregation in Human Blood Serum. Biomacromolecules. 2010;11(11):2836-2839. doi:10.1021/bm100971q
- 19. Shannahan JH, Lai X, Ke PC, Podila R, Brown JM, Witzmann FA. Silver Nanoparticle Protein Corona Composition in Cell Culture Media. PLoS ONE. 2013;8(9):e74001. doi:10.1371/journal.pone.0074001
- 20. Kokkinopoulou M, Simon J, Landfester K, Mailänder V, Lieberwirth I. Visualization of the protein corona: towards a biomolecular understanding of nanoparticle-cell-interactions. Nanoscale. 2017;9(25):8858-8870. doi:10.1039/c7nr02977b
- 21. Filipe V, Hawe A, Jiskoot W. Critical Evaluation of Nanoparticle Tracking Analysis (NTA) by NanoSight for the Measurement of Nanoparticles and Protein Aggregates. Pharmaceutical Research. 2010;27(5):796-810. doi:10.1007/s11095-010-0073-2
- 22. Winzen S, Schoettler S, Baier G, et al. Complementary analysis of the hard and soft protein corona: sample preparation critically effects corona composition. Nanoscale. 2015;7(7):2992-3001. doi:10.1039/c4nr05982d

- 23. Weber C, Morsbach S, Landfester K. Possibilities and Limitations of Different Separation Techniques for the Analysis of the Protein Corona. Angewandte Chemie International Edition. 2019;58(37):12787-12794. doi:10.1002/anie.201902323
- 24. Bannon MS, López Ruiz A, Corrotea Reyes K, et al. Nanoparticle Tracking Analysis of Polymer Nanoparticles in Blood Plasma. Particle & Particle Systems Characterization. 2021;38(6):2100016. doi:10.1002/ppsc.202100016
- 25. Ai Y, Gunawardena HP, Li X, Kim Y-I, Dewald HD, Chen H. Standard-Free Absolute Quantitation of Antibody Deamidation Degradation and Host Cell Proteins by Coulometric Mass Spectrometry. Analytical Chemistry. 2022;94(36):12490-12499. doi:10.1021/acs.analchem.2c02709
- 26. Ai Y, Xu J, Gunawardena HP, Zare RN, Chen H. Investigation of Tryptic Protein Digestion in Microdroplets and in Bulk Solution. Journal of the American Society for Mass Spectrometry. 2022;33(7):1238-1249. doi:10.1021/jasms.2c00072
- 27. Pochapski DJ, Carvalho Dos Santos C, Leite GW, Pulcinelli SH, Santilli CV. Zeta Potential and Colloidal Stability Predictions for Inorganic Nanoparticle Dispersions: Effects of Experimental Conditions and Electrokinetic Models on the Interpretation of Results. Langmuir. 2021;37(45):13379-13389. doi:10.1021/acs.langmuir.1c02056
- 28. Chen F, Wang G, Griffin JI, et al. Complement proteins bind to nanoparticle protein corona and undergo dynamic exchange in vivo. Nature Nanotechnology. 2017;12(4):387-393. doi:10.1038/nnano.2016.269
- 29. Blume JE, Manning WC, Troiano G, et al. Rapid, deep and precise profiling of the plasma proteome with multi-nanoparticle protein corona. Nature Communications. 2020;11(1)doi:10.1038/s41467-020-17033-7

- 30. Bantscheff M, Boesche M, Eberhard D, Matthieson T, Sweetman G, Kuster B. Robust and Sensitive iTRAQ Quantification on an LTQ Orbitrap Mass Spectrometer. *Molecular & amp;* Cellular Proteomics. 2008;7(9):1702-1713. doi:10.1074/mcp.m800029-mcp200
- 31. Keshishian H, Burgess MW, Specht H, et al. Quantitative, multiplexed workflow for deep analysis of human blood plasma and biomarker discovery by mass spectrometry. *Nature Protocols*. 2017;12(8):1683-1701. doi:10.1038/nprot.2017.054
- 32. Moman RN, Gupta N, Varacallo M. Physiology, Albumin. StatPearls Publishing Copyright © 2023, StatPearls Publishing LLC.; 2023.
- 33. Merlot AM, Kalinowski DS, Richardson DR. Unraveling the mysteries of serum albumin—more than just a serum protein. Mini Review. Frontiers in Physiology. 2014-August-12 2014;5doi:10.3389/fphys.2014.00299
- 34. Liu J, Wang Y, Xiong E, et al. Role of the IgM Fc Receptor in Immunity and Tolerance. Review. Frontiers in Immunology. 2019-March-22 2019;10doi:10.3389/fimmu.2019.00529
- 35. Miyakis S, Giannakopoulos B, Krilis SA. Beta 2 glycoprotein I--function in health and disease. Thromb Res. 2004;114(5-6):335-46. doi:10.1016/j.thromres.2004.07.017
- 36. McPherson HR, Duval C, Baker SR, et al. Fibrinogen αC-subregions critically contribute blood clot fibre growth, mechanical stability, and resistance to fibrinolysis. eLife. 2021;10doi:10.7554/elife.68761
- 37. Mirshafiee V, Kim R, Mahmoudi M, Kraft ML. The importance of selecting a proper biological milieu for protein corona analysis in vitro: Human plasma versus human serum. The International Journal of Biochemistry & Cell Biology. 2016/06/01/ 2016;75:188-195. doi:https://doi.org/10.1016/j.biocel.2015.11.019